



Article

Molecular Imprinting of Benzylpiperazine: A Comparison of the Self-Assembly and Semi-Covalent Approaches

Kathleen M. Wright^{1,2}, Michael C. Bowyer³, Adam McCluskey²  and Clovia I. Holdsworth^{2,*} 

¹ Sanitarium Health Food Company, 1 Sanitarium Drive, Berkeley Vale, NSW 2261, Australia

² School of Environmental and Life Sciences, University of Newcastle, Callaghan, NSW 2308, Australia

³ Academic Division, University of Newcastle, Ourimbah, NSW 2258, Australia

* Correspondence: clovia.holdsworth@newcastle.edu.au; Tel.: +61-2-4921-5481

Abstract: Molecularly imprinted polymers (MIPs) for benzylpiperazine (BZP, **1**), an illicit designer drug, were developed by using both self-assembly and semi-covalent approaches. From an array of potential functional monomers (FMs) and using a combination of pre-synthetic interaction studies (by molecular modelling and NMR analysis) and binding assays, the highest performing self-assembly 1-MIPs were confirmed to result from methacrylic acid (**7**) as FM, ethylene glycol dimethacrylate (EGDMA) or trimethylolpropane trimethacrylate (TRIM) as crosslinkers and chloroform as the porogen and rebinding solvent at template (T): FM ratios of 1:1 and 1:2, giving imprinting factors (IF) 3 to 7. The semi-covalent 1-MIPs were designed using benzylpiperazine (4-vinylphenyl) carbamate (**16**) as the template–monomer adduct in combination with either EDGMA or TRIM. Our comparative analysis showed the semi-covalent polymers to have a stronger affinity for **1** (significantly lower K_d values and higher IFs) and faster uptake than the self-assembly systems. Both approaches have comparable cross-reactivity: marginal to low against cocaine (**17**) and morphine (**18**) and high against ephedrine (**19**) and phenylpiperazine (**20**). They also have comparable selectivity: highly selective towards **1** against **17**, moderate against **18** and non-selective against **19**. EGDMA-based self-assembly MIPs displayed a greater imprinting effect (higher IFs and NIP-to-MIP K_d ratios) than TRIM-based MIPs, while the TRIM-based semi-covalent MIP outperformed its EGDMA-based equivalent. By virtue of its modest selectivity against the test illicit drugs, 1-MIPs could potentially be used as a dummy MIP for the broad-based capture and enrichment of illicit drug blends for subsequent laboratory analysis.

Keywords: molecular imprinting; molecularly imprinted polymers; MIP; self-assembly MIP; semi-covalent MIP; benzylpiperazine; benzylpiperazine MIP



Citation: Wright, K.M.; Bowyer, M.C.; McCluskey, A.; Holdsworth, C.I. Molecular Imprinting of Benzylpiperazine: A Comparison of the Self-Assembly and Semi-Covalent Approaches. *Int. J. Mol. Sci.* **2023**, *24*, 5117. <https://doi.org/10.3390/ijms24065117>

Academic Editor: Barbara Jachimska

Received: 19 January 2023

Revised: 2 March 2023

Accepted: 4 March 2023

Published: 7 March 2023



Copyright: © 2023 by the authors. Licensee MDPI, Basel, Switzerland. This article is an open access article distributed under the terms and conditions of the Creative Commons Attribution (CC BY) license (<https://creativecommons.org/licenses/by/4.0/>).

1. Introduction

Benzylpiperazine (BZP, **1**) is one of the dominant bioactive compounds in a relatively new class of piperazine-based illicit designer drugs in circulation [1]. This compound family includes 1-(3,4-methylenedioxyphenyl)piperazine (**2**), 1-(3-trifluoro-methylphenyl)piperazine (**3**), 1-(3-chlorophenyl)piperazine (**4**) and 1-(4-methoxyphenyl)piperazine (**5**) (Figure 1). The 1-hydrochloride salt (its most widely distributed form) is a white powder that is usually sold as tablets or capsules. It acts as a stimulant, increasing blood pressure, auditory vigilance and heart rate [2]. The biological activity of **1** is thought to be mediated through 5-HT-uptake inhibition and 5-HT1 antagonism effects [2–5]. Co-administration of **1** with **3** results in psychoactive effects, including hallucinations, similar to those associated with 3,4-methylenedioxymethamphetamine (MDMA), and is 10 times more active than amphetamine [6,7]. Ingestion of **1** can have lethal outcomes [8,9]. Increasingly, countries have listed **1** as an illicit substance, but up until 2008, **1** was legally available to people over the age of 18 in United Kingdom and New Zealand [10,11].

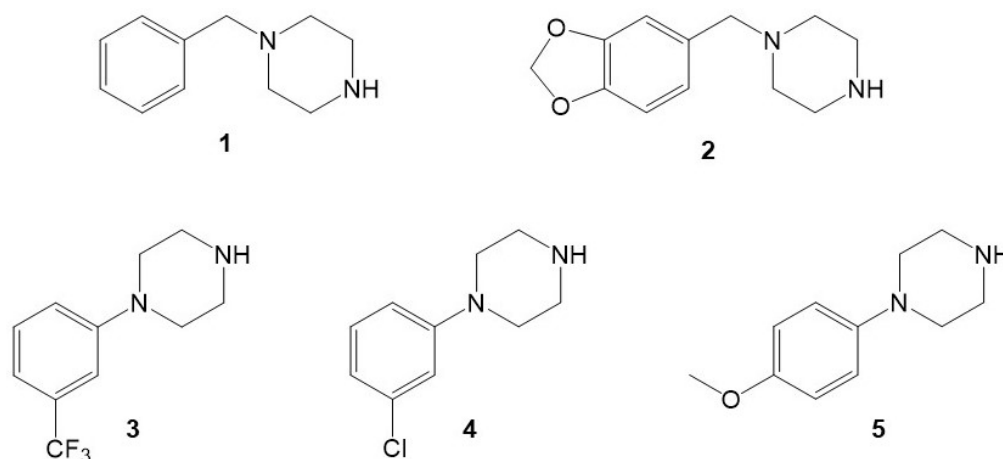


Figure 1. Chemical structures of benzylpiperazine (**1**) and its related analogues 1-(3,4-methylenedioxyphenyl)piperazine (**2**), 1-(3-trifluoromethylphenyl)piperazine (**3**), 1-(3-chlorophenyl)piperazine (**4**) and 1-(4-methoxyphenyl)piperazine (**5**).

A laboratory-based analyses of **1** could easily be conducted by using spectroscopic and chromatographic techniques [12,13], but reports on potential on-site detection have been limited to electrochemical methods [14,15] and presumptive colour tests [12,16]. While presumptive colour tests are rapid and cheap, these are prone to false positives, some tests are pH dependent and reagents have limited stability even with low temperature storage. Electrochemical methods rely on nonportable instrumentation with lower resolution than the chromatographic techniques. Spectroscopic on-site analysis is now possible with the emergence of portable instruments, e.g., FTIR; however, this would still require specialised training, as with all other forms of laboratory-based analytical instrumentation.

Molecular imprinted polymers (MIPs) have been used by our group [17,18] and others [19] for the capture and detection of illicit drugs. Nevertheless, there has been no report in the literature on MIPs designed for the capture of **1** to date. Thus, in this study, we aimed to develop **1**-selective MIPs, initially as an extraction and enrichment material and potentially as an on-site detection system. MIPs are generated from a functional monomer (FM), an analyte used as a template (T)—**1** in this study, a crosslinker (XL) for structural rigidity and a porogen (solvent) usually by radical polymerisation. Post-synthesis template extraction develops a complementary binding site within the polymer matrix, allowing highly selective analyte [20] or related analogue rebinding, i.e., dummy templating [21]. Due to their ease of synthesis, high stability and low cost, the use of MIPs as detection elements for several sensing platforms [22–25] is gaining momentum. At their simplest, MIPs are used as highly specific solid-phase extraction systems and afford easy identification and quantification by traditional analytical means [26–31].

Here we report on our efforts towards the development of a **1**-selective MIP via self-assembly and semi-covalent approaches. Being synthetically simpler, a majority of MIPs fall into the former classification. With self-assembly MIPs, the FM, T, XL and porogen are pre-mixed and allowed to self-associate prior to polymerisation. To optimise the formulation, pre-synthetic approaches such as virtual imprinting [32–34], semi-empirical calculations [11], thermodynamic studies [35,36], spectroscopic (NMR [37,38], UV–VIS [39,40] and FTIR [41]) analyses, chemometric methods [42] and combinatorial screening [33,43,44] have been extensively employed. Commercially available FMs are commonly utilised, except in cases where specialty monomers are required. Covalent and semi-covalent MIPs, on the other hand, require the formation a T-FM adduct, which, at times, involves numerous synthetic steps. Regardless, the covalent (T attached covalently to FM moiety during binding) and semi-covalent (T-FM interaction during rebinding is non-covalent, as with the self-assembly systems) approaches have been highly successful, especially in cases where the parent template was poorly functionalised and thus offered limited possibilities for strong

non-covalent interactions at the pre-polymerisation stage of MIP synthesis [45–47]. Our self-assembly MIP development process commenced with molecular modelling interaction and NMR titration (MM-NMR) studies to screen potential FMs and XLs (Figure 2) and determine the optimal FM-T interactions [17,18]. In the case of the semi-covalent approach, we synthesised and employed *O*-4-vinyl 4-benzylpiperazine-1-carbothioate (benzylpiperazine (4-vinylphenyl) carbamate, **16**, Figure 5) as a covalent surrogate for **1**.

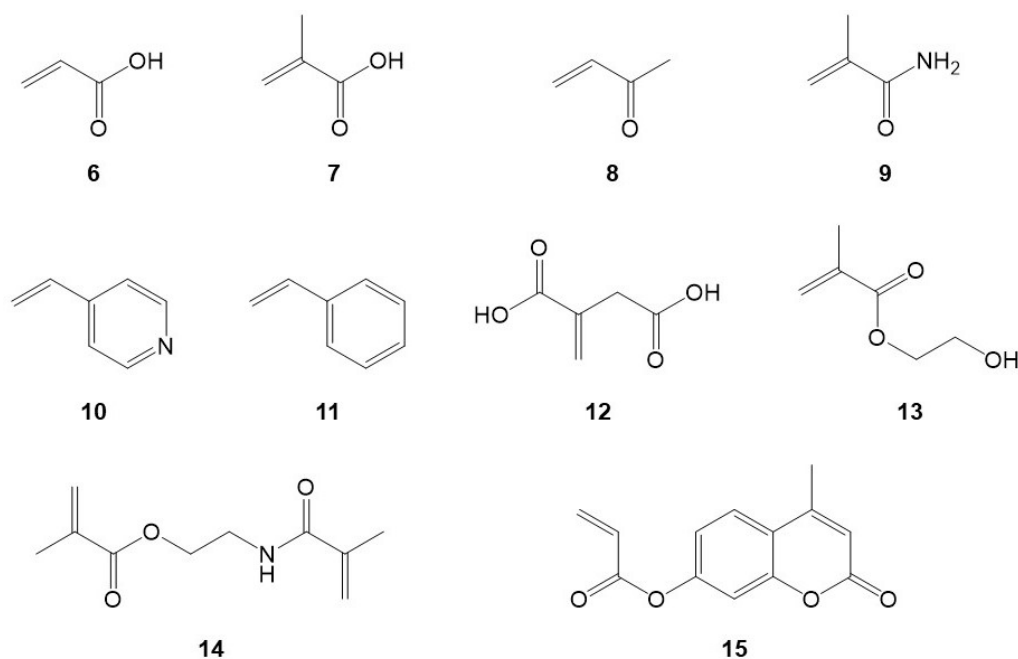


Figure 2. Chemical structures of functional monomers examined in this study: acrylic acid (**6**), methacrylic acid (**7**), acrylamide (**8**), methacrylamide (**9**), 4-vinylpyridine (**10**), styrene (**11**), itaconic acid (**12**), 2-hydroxyethyl methacrylate (**13**), *N,O*-bismethacroyloyl ethanolamine (NOBE) (**14**) and 7-hydroxy-4-methylcoumarin acrylate (**15**).

We successfully prepared high-performing self-assembly **1**-MIPs from methacrylic acid (**7**, Figure 2) as an FM, at T:FM ratios of 1:1 and 1:2, using chloroform as a porogen (IF's 3 to 7), with the EGDMA-based MIPs outperforming the TRIM MIPs. Nevertheless, the semi-covalent MIPs, particularly the TRIM-based polymers, have a stronger affinity for **1** (significantly lower K_d values and higher IFs) and faster uptake than the self-assembly systems. Both approaches exhibited comparable cross-reactivity—marginal to low against cocaine (**17**) and morphine (**18**) and high against ephedrine (**19**) and phenylpiperazine (**20**); and selectivity—highly selective towards **1** against **17**, moderate against **18** and non-selective against **19** (see Figure 7 for structures of test illicit substances).

An initial analysis might suggest that these high levels of cross-reactivity and modest selectivity against the tested illicit drugs were unfavourable; however, these **1**-templated MIPs are useful for broad-based capture and enrichment of illicit substances usually blended with, rather than specifically for, **1**, analogous to dummy-templated MIPs.

2. Results

2.1. The Self-Assembly Approach

2.1.1. Template–Monomer Interaction Studies

Molecular modelling (MM) analysis (Supplementary Figures S1–S5) identified potentially favourable hydrogen bond interactions (<2.8 Å) [48] between **1**, by virtue of the nitrogens of the piperazine ring, and the FMs **6**, **7** and **12–15** (see Figure 2 for FM structures) at **1**-FM ratios <1:2. Subsequent **1**-FM NMR interaction studies, i.e., ^{13}C NMR titration and Job plots (Supplementary Figures S9–S15), showed minimal or unfavourable interaction with **13–15**, but they did confirm favourable interactions with **6**, **7** and **12** at **1**-FM ratios <1:2.

These interactions were demonstrated by significant upfield shifts in the resonance signals (2.5–6 ppm) of the carbons in the piperazine ring of **1** in the presence of FMs **6**, **7** and **12**. The resonance shifts could be attributed to the hydrogen-bond interactions between the adjacent nitrogens and the acidic moieties of the FMs. Conversely, the carbonyl carbons of FMs **6**, **7** and **12** also exhibited a downfield movement (deshielding) of their signals, an expected effect of the hydrogen-bond interactions. The Job plots generated for **1** and FMs **6**, **7** and **12** also showed well-defined 1:1 stoichiometries (Supplementary Figures S9–S11), further confirming favourable 1-FM interactions.

Although some interaction between **1** and our selected XL agents, ethylene glycol dimethylacrylate (EGDMA), trimethylolpropane trimethylacrylate (TRIM) and divinylbenzene (DVB), were noted from computer simulations (Supplementary Figures S6–S8), ¹³C-NMR titration experiments presented very minimal 1-XL interactions (Supplementary Figures S14 and S15), making them ideal for promoting 1-FM association and the formation of template imprints.

2.1.2. Selection of Crosslinker

XL makes up about 80% of a MIP formulation and potentially has the greatest influence on non-specific binding in MIPs. Thus, to further our molecular modelling and NMR studies, the affinity of **1** to EGDMA, TRIM and DVB polymers was measured. These crosslinked polymers were prepared in the absence of **1** and any FM in acetonitrile (AN) and CHCl₃, the chosen porogens for 1-MIPs. Although **14** has been successfully used both as a functional monomer and crosslinker in OmniMIPs [49] and our MM and NMR data suggest that it could potentially work as a crosslinker (though not as a functional monomer) for 1-MIP, we excluded **14** in this study. High levels of non-specific binding of **1** were observed in DVB polymers, two to four times higher than in EDGMA and TRIM polymers. Of the three crosslinkers, only DVB is capable of π - π stacking interaction with **1**, and this is most likely the reason for the observed high level of superficial binding of **1**.

2.1.3. Preparation of 1-MIPs

Having identified **6**, **7** and **12** as suitable FMs from MM and NMR studies, the corresponding 1-MIPs were prepared in T:FM ratios of 1:1, 1:2 and 1:4 in CH₃CN and CHCl₃ as porogens and EGDMA and TRIM as crosslinkers. The T:FM ratios of 1:1 and 1:2 were chosen as per our MM and NMR results, showing the most favourable interaction between **1** and FMs **6**, **7** and **12** at these ratios. The 1:4 T:FM ratio is the most common ratio used in the literature to promote T-FM interactions and complex formation. The 1-MIPs were prepared in acetonitrile and chloroform to determine the effect of porogen polarity on the binding capabilities of the MIPs. Similarly, the influence of the level of crosslinking on the binding efficiency of 1-MIPs was also evaluated by employing di- (EGDMA) and tri-(TRIM) XLs.

All 36 formulations of 1-MIPs were prepared using 7 mL of porogen (~1 mmol FM + XL per 1 mL), with AIBN as the initiator, at 60 °C for 12 h. The resulting MIPs were ground with the fraction 32–63 μ m collected and Soxhlet extracted with 10% acetic acid in methanol, followed by pure methanol. Extraction was repeated until **1** could no longer be detected in the HPLC trace of the methanol extract.

Subsequent reference to these 1-MIP formulations follows the following codes: E and T for EGDMA and TRIM XLs, respectively; **6**, **7** and **12** for the corresponding FM, 1, 2 or 4 for 1:1, 1:2 and 1:4 T:FM ratios, respectively; and CH₃CN or CHCl₃ for the porogens. Thus, E7_{1-MIP}CHCl₃ refers to a 1-MIP prepared using EGDMA as XL and **7** as FM in a 1:1 T:FM ratio, with chloroform as the porogen.

2.1.4. Physical Characterisation

Scanning electron microscopy was used to examine the surface morphology of both MIPs and NIPs (non-imprinted polymer). No significant difference in surface morphology was observed between MIPs and their corresponding NIPs. MIP surface morphology

was unaffected by variations in the FM or T:FM ratio, but differences based on XL were apparent (Supplementary Figures S16 and S17). The TRIM-based MIPs appeared to be more compact, more dense and less porous than the surface of the EGDMA crosslinked polymers (Supplementary Figure S18). This was consistent with previous reports, which indicate that the nature of the crosslinker can affect polymer surface morphology [50]. It is also clear from Figure 3 that using CH₃CN as the porogen produced a macroporous surface morphology, while CHCl₃ produced smoother, more dense surfaces with fewer visible pores. This most likely resulted from a delayed phase separation from CHCl₃; that is, the growing polymer was more soluble in CHCl₃ than in CH₃CN, a product of solvent–polymer polarity mismatch [51]. The porogen effect on morphology was evident in swelling experiments, wherein all CHCl₃ polymers displayed an enhanced swelling capacity relative to the equivalent CH₃CN polymers.

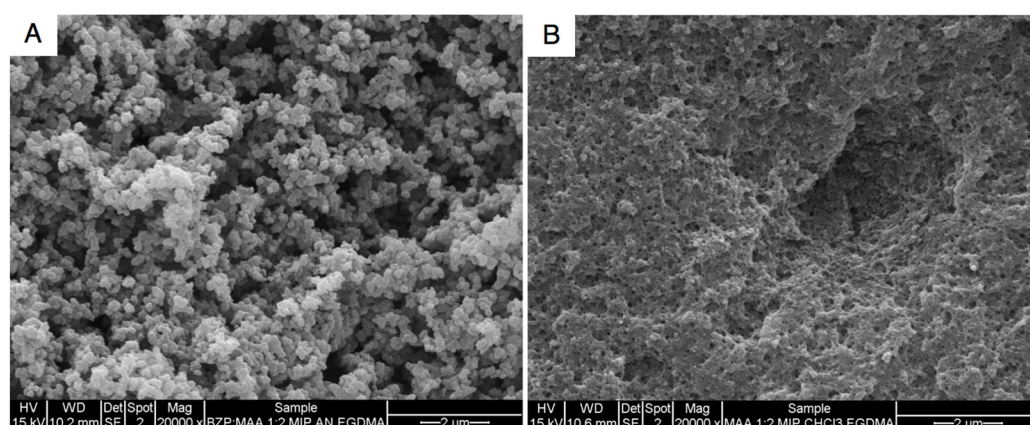


Figure 3. SEM images for (A) E7₂-MIP_{CH₃CN} and (B) E7₂-MIP_{CHCl₃} obtained at 20,000× magnification, at 15.0 kV.

2.1.5. Evaluation of the Imprinting Effect

The rebinding of **1** was initially evaluated by batch adsorption experiments, using 0.8 mM solution of **1** in CH₃CN or CHCl₃ with 30 min exposure to polymers of various masses (5, 10, 20 and 30 mg). As expected, the rebinding capacity was a function of the polymer mass used, typically plateauing at 20–30 mg polymer loading and increasing with increasing proportion of FM for both MIPs and NIPs. Our data suggest that the rebinding of **1** was not affected by the nature of the crosslinker; instead, it was porogen and FM dependent. In all instances, higher rebinding was observed with the CH₃CN MIPs, but the imprinting effect was enhanced in CHCl₃ MIPs, as a consequence of lower NIP rebinding of **1**.

This initial rebinding assays allowed us to screen MIPs and select those with an imprinting efficacy or imprinting factor IF (MIP binding/NIP binding) of ≥ 2 for all mass loadings for further binding characterisation. This imprinting efficacy criterion was obtained with MIPs E7₁-MIP_{CHCl₃}, E7₂-MIP_{CHCl₃}, T7₁-MIP_{CHCl₃} and T7₂-MIP_{CHCl₃}, with CHCl₃ as binding solvent; and E7₁-CH₃CN, bound in CH₃CN (Figure 4). Template uptake by these polymers varied from 17 to 75% and from 3 to 26% across the MIPs and their corresponding NIPs, respectively.

2.1.6. Binding Isotherms

The minimum time required to reach optimal template binding for MIPs E7₁-MIP_{CHCl₃}, E7₂-MIP_{CHCl₃}, T7₁-MIP_{CHCl₃} and T7₂-MIP_{CHCl₃} was determined prior to undertaking any other binding assays. No marked difference in the rebinding of **1** was observed for incubation times between 30 min and 24 h. Thus, we opted to use 60 min for subsequent binding tests. As only one MIP from the CH₃CN series (E7₁-CH₃CN) exhibited noteworthy imprinting, no further analysis of this series was undertaken.

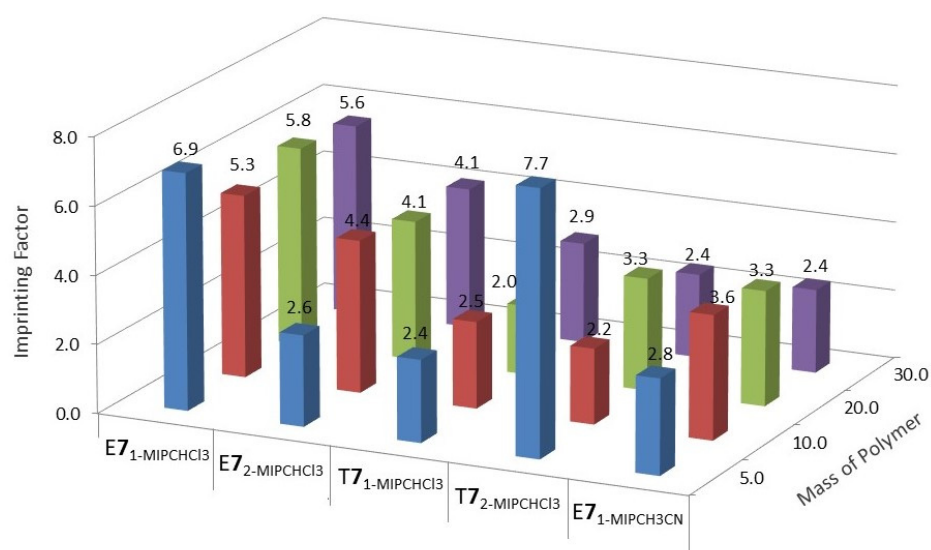


Figure 4. Imprinting factors (IFs) for the better-performing 1-MIPs (≥ 2) from the set of formulations utilising **6**, **7** and **12** as FMs, EGDMA and TRIM as XLs and CH₃CN and CHCl₃ as porogens. Rebinding studies were conducted using 1 mL of 0.8 mM solution of benzylpiperazine in the original porogen, with the uptake measured after 30 min. All binding tests were performed in triplicate.

The binding isotherms were generated by varying the rebinding solution concentration of **1** between 0.5 and 10 mM, using a constant polymer loading of 20 mg and 60 min incubation (Supplementary Figure S19A–D). Maximum binding (B_{\max}) and affinity constants (K_d) were calculated from non-linear regression of the Langmuir binding isotherms, using GraphPad Prism 9.4.1; the best-fit values obtained from the one-site-total-binding equation are presented in Table 1. These data show MIPs bound twice the amount of **1** than their corresponding NIPs, and this is attributable to the imprinting effect. E7₂ and T7₂ polymers (MIPs and NIPs) bound twice the amount of **1** than E7₁ and T7₁ polymers, a result that is unsurprising given that the E7₂ and T7₂ feed formulations contain twice the amount of functional monomer **7**.

Table 1. Binding and thermodynamic parameters for E7₁-MIPCHCl₃, E7₂-MIPCHCl₃, T7₁-MIPCHCl₃ and T7₂-MIPCHCl₃ towards **1**.

Polymers		K_d (μM)	B_{\max} ($\mu\text{mol/g}$)	K_d Ratio (NIP/MIP)	R^2
E7 ₁ -MIPCHCl ₃	MIP	0.27 ± 0.07	56.2 ± 5.6	5.0	0.966
	NIP	1.36 ± 0.83	30.0 ± 10.4		0.884
E7 ₂ -MIPCHCl ₃	MIP	0.22 ± 0.04	111.7 ± 9.3	4.5	0.988
	NIP	0.98 ± 0.50	66.2 ± 19.3		0.909
T7 ₁ -MIPCHCl ₃	MIP	0.60 ± 0.16	45.9 ± 6.0	2.5	0.933
	NIP	1.52 ± 0.73	22.7 ± 6.3		0.934
T7 ₂ -MIPCHCl ₃	MIP	0.31 ± 0.07	90.1 ± 9.7	2.3	0.984
	NIP	0.71 ± 0.26	35.7 ± 7.2		0.937
E16 _{MIP} CHCl ₃	MIP	0.09 ± 0.02	16.8 ± 1.2	-	0.949
T16 _{MIP} CHCl ₃	MIP	0.02 ± 0.01	21.5 ± 1.7	-	0.869

K_d and B_{\max} are the best-fit values at 95% confidence interval from non-linear regression of the binding isotherms (Supplementary Figure S19), using the one-site-total-binding equation generated using GraphPad Prism 9.4.1.

The K_d values for the MIPs (0.22–0.62 μM) were consistently lower than the corresponding NIPs (0.71–1.52 μM) because of the higher affinity template binding arising from the imprinting process. Furthermore, the K_d values were higher for the 1:1 (E7₁ and T7₁)

than for the 1:2 (E7₂ and T7₂) formulations, suggesting that the affinity for **1** was stronger at a higher functional monomer content. The NIP-to-MIP K_d ratios were higher for the EGDMA-based polymers (~5) than for the TRIM-based polymers (~2) and were consistent with the rebinding results and imprinting factors presented in Figure 4.

2.2. The Semi-Covalent Approach

The semi-covalent imprinting of **1** was undertaken by using *O*-4-vinyl 4-benzylpiperazine-1-carbothioate or benzylpiperazine (4-vinylphenyl) carbamate (**16**) as the template–monomer (TM) adduct (Figure 5 and Scheme 1). Post-polymerisation cleavage of the carbothioate linker would yield a proximally spaced phenol moiety capable of rebinding to **1** through hydrogen bonding upon re-exposure. The 4-vinylphenol moiety was previously utilised in the imprinting of cholesterol [52], *N*-heterocycles [53], profenofos and carbifuran [54] and substituted phenols [55].

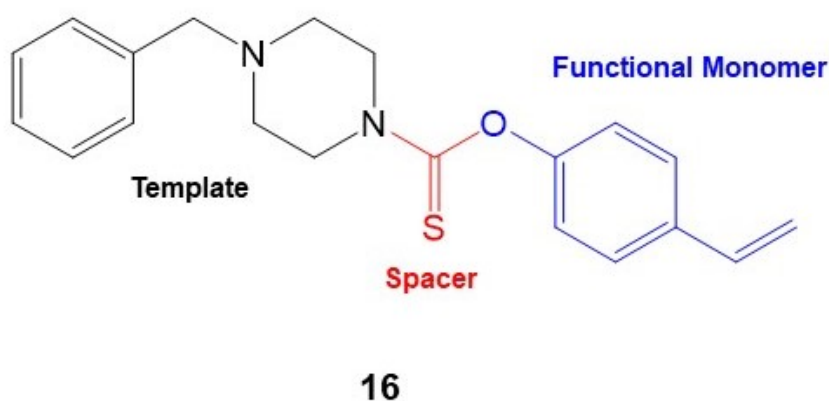
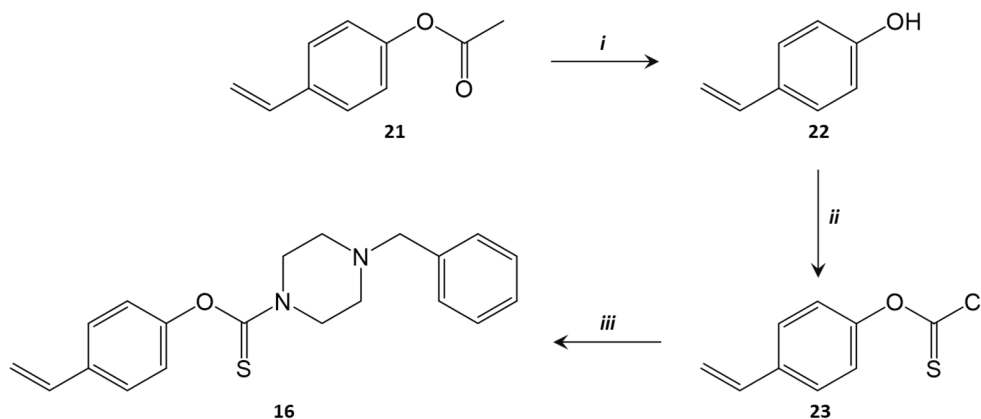


Figure 5. Chemical structure of *O*-4-vinyl 4-benzylpiperazine-1-carbothioate or benzylpiperazine (4-vinylphenyl) carbamate (**16**).



Scheme 1. Reagents and conditions: (i) KOH and CO₂ (g), 0–5 °C; (ii) NaOH, thiophosgene (SCCl₂) and CHCl₃, 0 °C; and (iii) NaOH, 0 °C.

Having synthesized the TM adduct **16**, MIPs were prepared in a 1:19 **16**:XL (EGDMA and TRIM) ratio in chloroform to give E**16**_{MIPCHCl₃} and T**16**_{MIPCHCl₃}, respectively. The corresponding NIPs were prepared under identical conditions, using the XLs only.

SEM micrographs of the MIPs displayed clear evidence of a macroporous surface structure (Supplementary Figure S20) consistent with the surface structure expected from low-polarity solvents such as CHCl₃ [18,51,56–59]. Both E**16**_{MIPCHCl₃} and T**16**_{MIPCHCl₃} exhibited low levels of swelling, with volume increases of 3–4% only upon exposure to the porogen CHCl₃.

2.2.1. Evaluation of Imprinting Effect

E16_{MIPCHCl₃} and T16_{MIPCHCl₃} were evaluated for their ability to selectively rebind **1** by batch adsorption experiments, using 1 mL of 0.8 mM solution of **1** in CHCl₃ and an incubation time of 30 min (as with the self-assembly MIPs). Both MIPs displayed a steady increase in template rebinding as a function of increasing polymer loading (from 5 mg to 30 mg), as is consistent with binding-site homogeneity [60]. The NIPs, on the other hand, displayed minimal binding, and this only slightly increased across all polymer loadings evaluated (Figure 6).

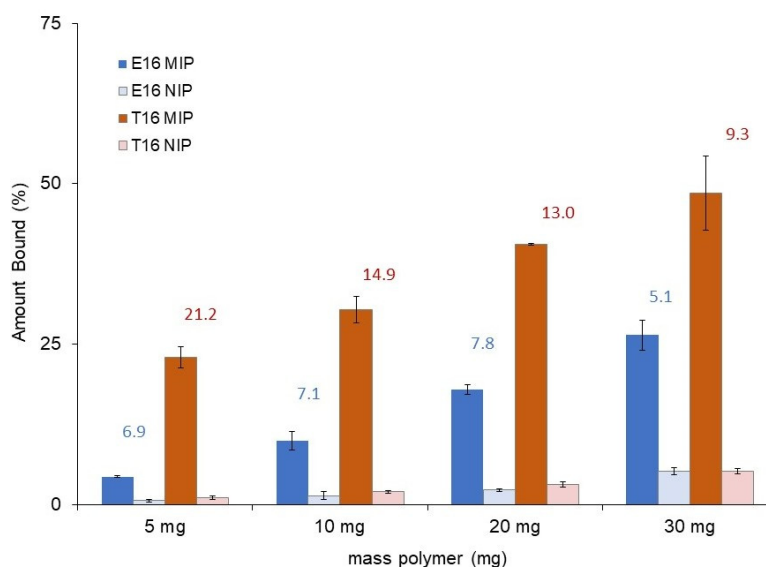


Figure 6. Rebinding results for E16_{MIPCHCl₃} and T16_{MIPCHCl₃} in CHCl₃, using 1 mL 0.8 mM solution of **1** with a binding time of 30 min. All experiments were performed in triplicate. Numerical values above the bars indicate imprinting factor (IF) values.

T16_{MIPCHCl₃} showed a greater affinity for **1**, binding at least twice the amount absorbed by E16_{MIPCHCl₃}, with maximum binding at 30 mg polymer loading, resulting in 49% and 26% uptake of **1**, respectively. This result is in keeping with previous reports suggesting that XLs with more than two polymerizable groups, such as TRIM, result in a more porous macrostructure with improved mass transfer properties (better access to the imprinted cavities) and higher capacities [61,62].

The imprinting effect, measured by the imprinting factor (IF; amount bound by MIP/amount bound NIP) ranged from 5.1 to 21, results consistent with the presence of well-defined **1**-specific cavities (Figure 6). It should be noted, however, that the NIPs lacked the FM component usually associated with NIP synthesis, as such, producing a poorer mimic on a non-imprinting effect, but nonetheless one that has been used in semi-covalent imprinting previously [52,63].

2.2.2. Binding Isotherms

Uptake of **1** was observed to be rapid, with optimal binding noted after 10 min for both MIPs. Binding isotherms (Supplementary Figure S19E) were generated across a 0.3–10 mM concentration range (of **1**) in CHCl₃, using 30 mg of polymer and a 60 min rebinding time in order to be consistent with the self-assembly systems. The binding constant, K_d , and B_{max} were calculated using non-linear regression of the Langmuir binding isotherms generated from GraphPad Prism, with the best-fit values obtained from the one-site-total-binding equation presented in Table 1. Since the NIPs showed negligible binding of **1**, only the MIPs were analysed. The K_d value for T16_{MIPCHCl₃} (0.02 μ M) is 5 times lower than E16_{MIPCHCl₃} (0.09 μ M), as is consistent with earlier observations (Figure 6) that the former has a greater affinity for **1**. These K_d values are also 3 and 33 times lower than the equivalent self-

assembly MIPs ($E7_{1-MIPCHCl_3}$ and $T7_{1-MIPCHCl_3}$), respectively. The binding capacities (B_{max}) of these semi-covalent MIPs are close in values and comparable to $T7_{1-MIPCHCl_3}$ but 3 times lower than $E7_{1-MIPCHCl_3}$.

2.3. Selectivity Studies

Both self-assembly ($E7_{1-MIPCHCl_3}$, $E7_{2-MIPCHCl_3}$, $T7_{1-MIPCHCl_3}$ and $T7_{2-MIPCHCl_3}$) and semi-covalent ($E16_{MIPCHCl_3}$ and $T16_{MIPCHCl_3}$) MIP systems were subjected to selectivity tests—single component (cross-reactivity) and binary competitive rebinding of **1** against cocaine (**17**), morphine (**18**), ephedrine (**19**) and phenylpiperazine (**20**) (Figure 7). These tests were conducted using 20 mg of polymer in 0.8 mM solutions of analyte in $CHCl_3$, with an incubation time of 60 min. A range of illicit drugs and precursors containing similar functionalities were chosen as competing analytes to simulate in-field capability for illicit detection.

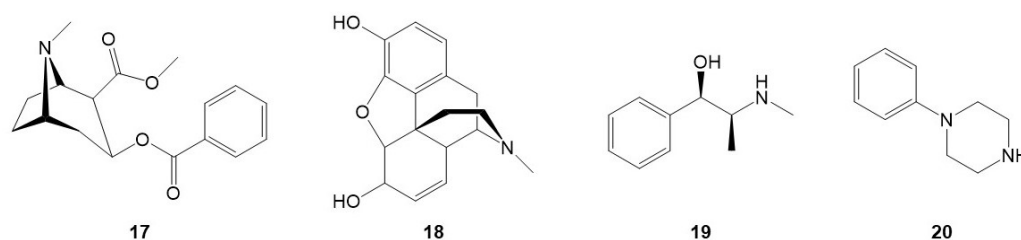


Figure 7. Chemical structures of illicit drugs used in competition and selectivity studies for **1**-based MIPs: cocaine (**17**), morphine (**18**), ephedrine (**19**) and phenylpiperazine (**20**).

2.3.1. Cross-Reactivity Tests

The results for the non-competitive cross-reactivity assays are given in Supplementary Figure S21, while Table 2 shows the cross-reactivity indices (XRF) to enable a direct comparison of the uptake of each competing analyte by the MIP with respect to **1**. The XRF for an analyte is defined as the ratio of the analyte (**17**, **18**, **19** or **20**) to **1** MIP binding within the MIP.

Table 2. Non-competitive cross-reactivity results for **1**-MIPs against cocaine (**17**), morphine (**18**), ephedrine (**19**) and phenylpiperazine (**20**).

MIP		1	17	18	19	20
$E7_{1-MIPCHCl_3}$	Bound (%) ¹	51.5 ± 3.4	6.7 ± 0.8	17.4 ± 3.1	74.5 ± 5.8	52.1 ± 4.9
	ΔB (%) ²	33.5 ± 2.9	−1.3 ± 1.8	5.4 ± 3.8	34.8 ± 6.2	27.8 ± 5.5
	XRF ³	1.00	0.13	0.34	1.44	1.01
$E7_{2-MIPCHCl_3}$	Bound (%)	82.9 ± 2.2	12.2 ± 2.7	19.4 ± 7.4	82.9 ± 2.4	74.2 ± 3.9
	ΔB (%)	45.6 ± 2.3	2.8 ± 2.1	3.3 ± 3.1	23.4 ± 2.5	35.3 ± 2.2
	XRF	1.00	0.15	0.23	1.00	0.90
$T7_{1-MIPCHCl_3}$	Bound (%)	43.3 ± 3.4	3.5 ± 1.1	18.5 ± 2.5	54.9 ± 1.2	35.8 ± 4.0
	ΔB (%)	31.4 ± 3.6	0.6 ± 2.3	9.0 ± 2.6	24.6 ± 1.2	14.2 ± 4.0
	XRF	1.00	0.08	0.43	1.27	0.83
$T7_{2-MIPCHCl_3}$	Bound (%)	76.4 ± 3.4	11.2 ± 1.2	20.5 ± 4.2	76.8 ± 4.0	62.3 ± 1.8
	ΔB (%)	52.1 ± 5.0	2.2 ± 1.2	7.0 ± 4.5	25.1 ± 4.1	35.0 ± 4.0
	XRF	1.00	0.15	0.27	1.01	0.82
$E16_{MIPCHCl_3}$	Bound (%)	26.3 ± 2.5	16.8 ± 0.7	11.0 ± 2.0	26.0 ± 2.2	18.9 ± 1.5
	ΔB (%)	17.5 ± 3.2	8.9 ± 1.4	1.5 ± 2.3	12.1 ± 2.2	14.0 ± 2.2
	XRF	1.00	0.64	0.42	0.99	0.72
$T16_{MIPCHCl_3}$	Bound (%)	53.0 ± 1.4	45.0 ± 1.5	16.4 ± 2.2	39.8 ± 2.2	34.8 ± 4.4
	ΔB (%)	48.5 ± 1.9	41.0 ± 1.6	8.5 ± 2.3	36.8 ± 4.6	32.1 ± 4.5
	XRF	1.00	0.85	0.31	0.75	0.66

¹ Rebinding studies were conducted by incubating 20 mg of polymer in 1 mL of 0.8 mM solution of analyte in $CHCl_3$ for 60 min. All binding tests were performed in triplicates. ² ΔB = MIP binding − NIP binding. ³ XRF = cross-reactivity factor = analyte MIP binding/template **1** MIP binding.

The four self-assembly MIPs (E7_{1-MIPCHCl3}, E7_{2-MIPCHCl3}, T7_{1-MIPCHCl3} and T7_{2-MIPCHCl3}) displayed high levels of cross-reactivity with **19** and **20**, with the XRFs ranging from 0.82 to 1.44, low to moderate with **18** (XRF = 0.23 to 0.43) and negligible with **17** (XRF = 0.08 to 0.15). Selective binding ($\Delta B = \text{MIP binding} - \text{NIP binding}$) followed the same trend. These results reflect the effect of functional group character (electronic, size), relative proximity and orientation on each analyte with respect to **1**. Analytes **17** and **18** are both large molecules that differ in shape, potential and available functional groups to **1**, leading to a poor 'fit' within the imprinted cavities (Supplementary Figure S22). Consequently, they displayed low sorption and low affinity to the MIPs. In contrast, **19** and **20** are similar in size and chemical character to **1**, consistent with the observed high XRFs (Supplementary Figure S23). The very high uptake of **19**, equivalent or higher than **1**, could be attributed to multipoint H-bonding interactions with the MAA FM by virtue of its NH and OH groups, which are H donor/acceptor species, leading to potentially greater binding affinity. Furthermore, analyte **19** is the only test target containing an amine unit that is not part of a ring system, which could mean greater fluxionality, resulting in better orientation within the binding cavity.

The semi-covalent MIPs (E16_{MIPCHCl3} and T16_{MIPCHCl3}) showed a cross-reactivity trend that is similar to the self-assembly MIPs, except for analyte **17**, which recorded high levels of cross-reactivity (XRF's 0.64 and 0.85 for E16_{MIPCHCl3} and T16_{MIPCHCl3}, respectively) in contrast to its behaviour towards the self-assembly MIPs. Note that the post-polymerisation cleavage of the carbothioate linker of **16** (Figure 5) to release the template moiety leaves a phenol functionality within the cavity capable of interacting with **1** or other complementary analytes. The XRFs for **19** and **20** are slightly lower than those observed with the self-assembly MIPs, thus suggesting a less favourable affinity to the imprinted cavities containing the phenol functionality than with the MAA carboxyl unit. The unexpected high cross-reactivity with **17** could possibly be due to its benzoyl group, which is similar in structure and size to the benzyl group of **1**, that could easily fit the imprinted cavities and interact with the phenol group by pi-pi stacking.

2.3.2. Binary Competitive Assays

The selectivity of the MIPs was further tested using binary mixtures of **1** and competing analytes **17**, **18** and **19**. Analyte **20** was not pursued in this assay due to HPLC separation issues with **1**.

The uptake of all analytes was observed to be higher for MIPs than in their corresponding NIPs (Supplementary Figure S24), thus suggesting that they have access to and an affinity for the imprinted cavities. To facilitate binding selectivity analysis, we introduced the quantitative values summarized in Table 3. First, the uptake of **1** as the sole analyte, a measure of the MIP binding capacity, is taken as a reference; the binding of binary analytes is then normalised against this reference. Thus, if the normalised binding of an analyte is greater than 1, i.e., greater than 100%, then this means that its uptake is higher than the expected binding capacity. The selectivity index (SI) of an analyte is defined here as the ratio of normalised analyte binding to normalised **1** binding.

Although selectivity assessment is more essential for MIPs than NIPs, and despite the fact that NIP binding could be variable due to its superficial nature, the results of this study showed analyte **19** to be competitive with **1** in all NIP systems, giving normalised binding values as high as 3.15. The binding of **17** and **18**, however, was always lower or equivalent to that of **1**. Uptake of **1** by the semi-covalent NIPs is lower than the reference in all cases, while self-assembly NIPs registered **1** binding higher than the reference in some binary mixtures.

Table 3. Binary competition results for 1-MIPs against cocaine (**17**), morphine (**18**) and ephedrine (**19**).

Polymer	Binding ¹	MIP				NIP			
		1	17	18	19	1	17	18	19
E7 ₁ -MIPCHCl ₃	Reference (%) ²	51.5 ± 3.4				18.0 ± 3.6			
	Normalised ³	1.09	0.19			1.19	0.41		
		1.05		0.38		0.77		0.38	
		0.94			1.73	0.66			2.50
SI ⁴	1.00	0.18	0.37	1.85	1.00	0.34	0.49	3.80	
E7 ₂ -MIPCHCl ₃	Reference (%)	82.9 ± 2.2				37.2 ± 3.1			
	Normalised	0.93	0.15			1.11	0.16		
		0.86		0.22		0.88		0.02	
		0.86			1.06	0.90			1.89
SI	1.00	0.16	0.26	1.23	1.00	0.14	0.02	2.11	
T7 ₁ -MIPCHCl ₃	Reference (%)	43.3 ± 3.4				11.9 ± 1.2			
	Normalised	1.12	0.18			1.90	0.56		
		1.24		0.20		1.64		0.56	
		0.74			1.29	1.15			3.15
SI	1.00	0.16	0.16	1.74	1.00	0.30	0.34	2.74	
T7 ₂ -MIPCHCl ₃	Reference (%)	76.4 ± 3.4				24.3 ± 3.6			
	Normalised	0.89	0.11			1.11	0.10		
		0.89		0.20		1.38		0.26	
		0.78			1.04	0.92			2.28
SI	1.00	0.12	0.23	1.32	1.00	0.09	0.19	2.47	
E16 _{MIPCHCl₃}	Reference (%)	26.3 ± 2.5				8.7 ± 2.0			
	Normalised	1.01	0.07			0.72	0.37		
		0.33		0.15		0.35		0.20	
		0.63			1.14	0.17			1.54
SI	1.00	0.07	0.46	1.81	1.00	0.51	0.59	8.85	
T16 _{MIPCHCl₃}	Reference (%)	53.0 ± 1.4				4.5 ± 1.3			
	Normalised	0.71	0.13			0.89	0.60		
		0.33		0.20		0.63		0.66	
		0.42			0.57	0.34			1.18
SI	1.00	0.18	0.61	1.34	1.00	0.68	1.05	3.50	

¹ Rebinding studies were conducted by incubating 20 mg of polymer in 1 mL of 0.8 mM solution of analyte in CHCl₃ for 60 min. All binding tests were performed in triplicates. ² Binding of **1** as sole analyte. ³ Binding of binary analytes with respect to reference. ⁴ SI = selectivity index = normalised analyte binding/normalised **1** binding.

In the case of MIPs, **19** was also observed to be highly competitive, reducing the uptake of **1** to a low of 0.42, i.e., 42% (T16_{MIPCHCl₃}), with respect to the reference and displayed normalised binding and SIs higher than **1** (as high as 1.73 and 1.85, respectively, with E7₁-MIPCHCl₃) in all cases. Analyte **18** displayed low levels of competition with **1** in the self-assembly MIPs (SI = 0.16 to 0.37), slightly reducing the binding of **1** in some cases. However, the presence of **18** brought about a significant reduction in **1** binding (below 50%), resulting in a moderate SI of 0.46 (E16_{MIPCHCl₃}) and 0.61 (T16_{MIPCHCl₃}) in the case of the semi-covalent MIPs. Analyte **17** did not have a significant impact on the binding of **1**, except in T16_{MIPCHCl₃}, and displayed low-to-minimal competition tendency against **1**, with normalized binding and SI values all being <0.2. In some instances (also observed with the NIPs), the presence of **17** and **18** enhanced the uptake of **1**, which could be attributed to its interaction with these analytes by hydrogen bonding and/or pi–pi stacking. On the other hand, in the presence of **19**, the uptake of **1** in all polymers tested was reduced, thus confirming its observed competitive tendency against **1**.

Consistent with the results of the non-competitive cross-reactivity assays, the results of the competitive (binary mixtures) binding studies showed all MIPs to be highly selective towards **1** in the presence of **17** (SI < 0.2), moderately selective in the presence of **18** (SI > 0.2 to ~0.6) and non-selective in the presence of **19** (SI > 1).

2.3.3. Selectivity of 1-MIPs: Implication on Their Applications

The poor-to-moderate selectivity of 1-MIPs against **18**, **19** and **20** could initially be construed as unfavourable; however, these results indicate that 1-MIPs are capable of broad-based capture of blends of illicit substances with, rather than specifically for, **1**, comparable to the 'dummy' MIP approach. The high cross-reactivity against **20** means that 1-MIPs could potentially extract 1-(3-trifluoromethyl-phenyl)piperazine (TFMPP, **3**), a derivative of **20** most commonly blended with **1**, and other known substituted phenylpiperazine blend ingredients such as **4**, **5** (Figure 1) and 4-fluorophenylpiperazine [64]. Other pills are also known to be mixed with cocaine (**17**) [16,65] and ephedrine (**19**) [64], which, according to our selectivity studies, could also be extracted by 1-MIPs.

Illicit drugs are never pure, and conducting an analysis of their composition, including minor ingredients and adulterants, is essential in drug profiling studies [66]. The competitive uptake of **18**, **19** and **20** by 1-MIPs means that, when present in trace amounts, they could be pre-concentrated within the MIP, which could enhance their detection. We speculate that other minor non-piperazine derivatives blended with **1** could also be captured and pre-concentrated with 1-MIPs. Unfortunately, due to the nature of these analytes, we could not easily obtain real samples to test.

Our results suggest no significant difference in the selectivity between self-assembly and semi-covalent 1-MIPs. Thus, the MIP materials could be prepared by the synthetically simpler self-assembly imprinting using cheap commercially available monomers (monomer **7** and crosslinkers), thus making these materials very competitive over other analytical extraction methods.

Our 1-MIP materials are suited to laboratory test setting, with potential as the recognition element for in-field sensing devices. Sample preparation would be simple, and with their enhanced enrichment capability, due to the presence of imprinted sites, they would be useful for the capture of illicit drugs, particularly in biological samples. MIP-bound drug analytes could be re-extracted and differentiated by a number of analytical procedures—notably, chromatographic methods—preferably with MS detection and capillary electrophoresis, among others.

3. Materials and Methods

3.1. Reagents

Benzylpiperazine (**1**) was purchased from Fluka and used as received. Azobisisobutyronitrile (AIBN) was obtained from DuPont and was recrystallised from acetone prior to use. Acrylic acid (**6**), methacrylic acid (**7**), itaconic acid (**12**), divinylbenzene (DVB), ethylene glycol dimethacrylate (EGDMA), trimethylolpropane trimethacrylate (TRIM), sodium hydroxide, glacial acetic acid, hydrochloric acid, potassium hydroxide, (1*R*, 2*S*)-(-)-ephedrine (**19**), 1-phenylpiperazine (**20**), p-acetoxystyrene (**21**), thiophosgene and 7-hydroxy-4-methylcoumarin were purchased from Sigma-Aldrich and used as received, unless otherwise stated. Monomers **6** and **7** and the crosslinkers DVB and EGDMA were distilled under reduced pressure prior to use. TRIM was purified by washing with aqueous sodium hydroxide (0.1 M, 2 × 50 mL), water (50 mL) and saturated brine solution (50 mL) and then dried over MgSO₄. *N,O*-bismethacryloyl ethanolamine (NOBE, **14**), 7-hydroxy-4-methylcoumarin acrylate (**15**) and benzylpiperazine (4-vinylphenyl) carbamate (**16**) were synthesized in-house, according to the synthetic procedures outlined below. Cocaine base (**17**) and morphine (**18**) was provided by the Australian Federal Police Forensic Services and was used as received. Methacryloyl chloride and acryloyl chloride were purchased from Fluka and Lancaster, respectively, and used as received.

HPLC-grade acetonitrile and chloroform were obtained from Merck and were used as received. All other solvents were distilled prior to use, unless otherwise stated.

Deuterated chloroform (99.8%) and dimethylsulfoxide (99.8%) for NMR analysis were obtained from Cambridge Isotope Laboratories Incorporated.

3.2. Preparation of *N,O*-Bismethacryloyl Ethanolamine (NOBE, **14**)

NOBE (**14**) was prepared as per the method utilised by Sibrian-Vazquez and Spivak [49]. Ethanolamine (0.976 g, 16 mmol) was mixed with 15 mL of dichloromethane. TEA (3.74 g, 5.15 mL, 37 mmol) was added in small portions to the initial mixture, with stirring, and the reaction mixture was cooled to 0 °C. Methacryloyl chloride (3.867 g, 3.6 mL, 37 mmol) was added dropwise, with vigorous stirring, while keeping the temperature at 0 °C. After the complete addition of methacryloyl chloride, the temperature was increased to 40 °C and allowed to react for 24 h at this temperature. The reaction mixture was filtered, and the precipitate (Et₃NHCl) was then discarded. The filtrate was extracted with 0.5 M NaHCO₃ (3 × 15 mL) and 0.5 M sodium citrate (3 × 15 mL). The solvent was evaporated under vacuum, the compound was isolated by column chromatography (EtOAc/hexanes 50:50, EtOAc 100%), and **14** was isolated as a pale yellow oil. Yield: 59%. ¹H NMR (CDCl₃, 300 MHz): δ/ppm = 6.80, 5.99, 5.71, 5.60, 5.38, 4.25, 3.58, 1.97, 1.89. ¹³C NMR (CDCl₃, 75.5 MHz): δ/ppm = 168.5, 167.4, 139.8, 135.9, 126.0, 119.4, 63.2, 39.0, 18.4, 18.1.

3.3. Preparation of 7-Hydroxy-4-methylcoumarin Acrylate (**15**)

First, **15** was prepared by the literature method [67]. TEA (12.1 g, 120 mmol) and 7-hydroxy-4-methylcoumarin (8.809 g, 50 mmol) were dissolved in chloroform (150 mL) and cooled to 0 °C. Acryloyl chloride (10.9 g, 120 mmol) was added dropwise, with vigorous stirring. The reaction mixture was then returned to room temperature and stirred for a further 12 h. The solvent was evaporated under vacuum, and the product was purified by dissolving the precipitate in methanol (200 mL). The methanol solution was then poured into water (1 L), the precipitate was collected by filtration, and **15** was isolated as a white flake. ¹H NMR (CDCl₃, 300 MHz): δ/ppm = 7.86, 7.39, 7.28, 6.67, 6.62, 6.52, 6.48, 6.24, 3.41. ¹³C NMR (CDCl₃, 75.5 MHz): δ/ppm = 163.8, 159.7, 153.6, 153.0, 152.6, 134.4, 127.3, 126.5, 118.4, 117.7, 113.9, 110.2, 18.2.

3.4. Synthesis of Benzylpiperazine (4-Vinylphenyl) Carbamate (**16**)

3.4.1. Synthesis of 4-Vinylphenol (**22**) [68]

4-Acetoxystyrene (**21**) (2.0 g, 13.22 mmol) was added to potassium hydroxide (2.0 g, 35.65 mmol) in water (25 mL) and stirred at 0–5 °C until homogeneous (5 h). Gaseous carbon dioxide was passed into the stirred cold solution to pH 8 to produce p-vinylphenol (**22**) [62]. Yield: 61%. ¹H NMR (CDCl₃, 300 MHz): δ 7.30, 6.79, 6.63, 5.54, 5.04. ¹³C NMR (CDCl₃, 75.5 MHz): δ 158.4, 137.6, 130.3, 128.4, 116.0, 110.9.

3.4.2. Synthesis of 4-Vinylphenyl Chlorothioformate (**23**) [69]

A solution of **22** (0.5 g, 4.2 mmol) in 5% NaOH (5 mL) was added dropwise, with stirring, to a solution of thiophosgene (0.45 g, 4.2 mmol) in chloroform (3 mL) cooled to 0 °C. The reaction was stirred for 1 h, at 0–5 °C, and the chloroform layer washed with dilute HCl and water. Solvent was removed under reduced pressure, and product **23** was separated by column chromatography (silica gel, 10% EtOAc:hexane). Yield: 85%. ¹H NMR (CDCl₃, 300 MHz): δ 7.46, 7.08, 6.67, 5.70, 5.26. ¹³C NMR (CDCl₃, 75.5 MHz): δ 185.7, 154.0, 136.8, 135.4, 127.6, 121.2, 120.9, 115.2.

3.4.3. Synthesis of *O*-4-Vinyl 4-Benzylpiperazine-1-carbothioate (**16**)

4-Vinylphenyl chlorothioformate (**23**) (0.7 g, 3.54 mmol) was added dropwise to **1** (1.25 g, 7.09 mmol), with stirring. The reaction was stirred for 1 h, and product **16** was separated by column chromatography (silica gel, 5% to 10% EtOAc:hexane). Yield: 40%. ¹H NMR (CDCl₃, 300 MHz): δ 7.30 (d), 7.21 (m), 6.89 (d), 6.58 (q), 5.60 (d), 5.13 (d), 4.09 (m), 3.88 (m), 3.50 (s), 2.51 (d) ppm. ¹³C NMR (CDCl₃, 75.5 MHz): δ 186.9, 153.4, 136.1, 135.7, 129.5, 128.7, 127.8, 127.1, 123.0, 114.3, 62.8, 52.6, 52.4, 50.2, 46.3.

3.5. Molecular Modelling

Template–monomer molecular interactions were modelled using Spartan '04 software, using the AM1 force field. This molecular orbital computational method predicts the stable configuration of the template (T), functional monomer (FM), FM-FM clusters and T-FM clusters and calculates their standard heats of formation (ΔH_f). The molecules were randomly positioned, and the T-FM clusters were modelled with respect to increasing the template–monomer ratio from 1 to 4. To account for the FM-FM interaction, the FM-FM clusters of up to five molecules were also surveyed. The energies of interaction of the T-M clusters, ΔE° (cluster), at different molecular ratios were then calculated using the following equation:

$$\Delta E_{\text{interaction}} = \Delta H_f \text{ FM-T complex} - [\Delta H_f \text{ monomer cluster} - \Delta H_f \text{ template}] \quad (1)$$

3.6. NMR Spectroscopic Analysis

^1H and ^{13}C Nuclear Magnetic Resonance (NMR) spectra were recorded at 300.13 and 75.47 MHz, respectively, using a Bruker Avance 300 MHz Spectrometer in conjunction with Bruker Topspin v1.3 software. Experiments involving **6**, **7** and **14** were performed in CDCl_3 , while experiments with **12** were performed in $\text{DMSO}-d_6$ at a temperature of 301 K. For the NMR titration, molar aliquots of monomer were sequentially added to the template **1** (0.1 mmol) up to a maximum of 16 equivalents. After each aliquot addition, the sample was mixed and allowed to spin for five minutes before spectrum acquisition. The experiment was repeated in the absence of **1**. For the Job experiments, 11 samples were prepared with varying **1** and monomer molar ratios, ranging from 0 to 1, using 0.2 mM solutions. The total volume was constant at 0.5 mL.

3.7. Polymer Synthesis and Template Extraction

3.7.1. Self-Assembly MIPs

The required amounts of functional monomer (0.34 mmol, 0.68 mmol or 1.36 mmol) and crosslinker (6.64 mmol, equivalent to $20 \times \text{T}$) were added to a solution of **1** (60 mg, 0.34 mmol) in 7 mL porogen (CH_3CN or CHCl_3). Based on our MM-NMR analysis, **6**, **7** and **12** were selected as functional monomers and EGDMA and TRIM as crosslinkers. MIPs were prepared using 1:1, 1:2 and 1:4 T:M ratios in chloroform and acetonitrile. The reaction mixture was degassed with N_2 before AIBN (50 mg) was added. The mixture was heated to 60 °C in an oven (Thermoline). NIPs were prepared by using the same method but without the addition of **1**.

Polymers were ground wet in methanol and sieved with the fraction between 32 and 65 μm collected. Template removal was by Soxhlet extraction, using a 10% acetic acid-methanol mix for 48 h, followed by 100% methanol for 12 h. The polymers were dried at 40 °C for 24 h.

3.7.2. Semi-Covalent MIPs

Benzylpiperazine(4-vinylphenyl)thiocarbamate (**16**) (115 mg, 0.34 mmol) was mixed with crosslinker (EGDMA or TRIM, 6.46 mmol) and AIBN (1% mol ratio) in chloroform (2 mL/g monomers). The reaction mixture was degassed with N_2 and then heated to 60 °C in an oven (Thermoline). NIPs were prepared using the same method but without the addition of **16**.

Polymers were ground wet in methanol and sieved with the fraction between 32 and 65 μm collected. The template adduct was cleaved by heating the polymer at reflux over 1 M NaOH for 12 h and then neutralised with dilute HCl. The polymers were then washed with methanol for 12 h, using a Soxhlet extractor. Finally, the polymers were dried at 40 °C for 24 h [48,49,55].

3.8. Batch-Binding Tests for **1**

3.8.1. HPLC Analytical Method

Batch rebinding experiments were carried out using a known concentration of **1** stock solution in either acetonitrile or chloroform. The required mass of polymer was left in contact with the **1** solution for the required time. The quantification of **1** was achieved by HPLC, using a Shimadzu High Performance Liquid Chromatograph (HPLC) (LC-20AD) fitted with an Econosphere™ C18, 5 μm column (Grace®).

For **1** binding in CH_3CN , the mobile phase comprised 50% CH_3CN and 50% buffer solution (25 mM K_2HPO_4 ; 30 mM KCl; 7 mM TEA; adjusted to pH 3 with H_3PO_4). A 10 μL injection volume was used with a run time of 10 min, flow rate of 2 mL min^{-1} and detection wavelength of 254 nm.

For binding in CHCl_3 , the mobile phase consisted of 70% CH_3CN and 30% buffer solution (25 mM K_2HPO_4 ; 30 mM KCl; 7 mM TEA; adjusted to pH3 with H_3PO_4). A 10 μL injection volume was used with a run time of 15 min, flow rate of 0.95 $\text{mL}\cdot\text{min}^{-1}$ and detection wavelength of 254 nm. A calibration curve was generated using six solutions in the range of 0.1 to 0.8 mM.

3.8.2. Sorption Tests: Evaluation of Imprinting Effect

A sorption study to evaluate the imprinting efficiency was performed. Various polymer masses from 10.0 to 30.0 mg were placed into 5 mL vials to which was added 1.00 mL of 0.0800 mM **1** in CH_3CN or chloroform. The mixture was shaken for 30 min, filtered and the filtrate analysed directly by HPLC. The amount of free **1** was subtracted from the initial binding solution concentration to obtain the amount of **1** bound in the polymer. All binding experiments for this study were performed in triplicate to ensure reproducibility.

Results of the sorption tests were favourable for only 4 of the self-assembly systems tested: $\text{E7}_1\text{-MIPCHCl}_3$, $\text{E7}_2\text{-MIPCHCl}_3$, $\text{T7}_1\text{-MIPCHCl}_3$ and $\text{T7}_2\text{-MIPCHCl}_3$ MIPs. The other systems were no longer pursued in subsequent studies.

3.8.3. Time-Binding Study

To a set of triplicates of 30.0 mg of self-assembly systems $\text{E7}_1\text{-MIPCHCl}_3$, $\text{E7}_2\text{-MIPCHCl}_3$, $\text{T7}_1\text{-MIPCHCl}_3$ and $\text{T7}_2\text{-MIPCHCl}_3$, and semi-covalent MIPs $\text{E16}_{\text{MIPCHCl}_3}$ and $\text{T16}_{\text{MIPCHCl}_3}$ polymers, 1.00 mL of 0.0800 mM **1** was added and the mixture shaken for a designated time of contact. The binding times investigated were 0.5, 2.0, 4.0, 7.0 and 18 h. After binding, the mixtures were filtered, and the filtrates were analysed by HPLC. The amount of bound **1** was then obtained by subtracting the amount of **1** left in solution from the initial concentration.

3.8.4. Saturation Binding

A series of 20.0 mg of self-assembly polymers $\text{E7}_1\text{-MIPCHCl}_3$, $\text{E7}_2\text{-MIPCHCl}_3$, $\text{T7}_1\text{-MIPCHCl}_3$ and $\text{T7}_2\text{-MIPCHCl}_3$ were incubated in different concentrations of **1** for 1 h, after which, the mixtures were filtered, and the filtrates were analysed directly by HPLC. The amount of bound **1** was then obtained by subtracting the amount of **1** left in solution from the initial concentration. Binding isotherms were generated from GraphPad Prism 9.4.1, and the best-fit values from non-linear regression, using the one-site-total-binding equation, were obtained.

The same procedure was followed for the semi-covalent MIPs $\text{E16}_{\text{MIPCHCl}_3}$ and $\text{T16}_{\text{MIPCHCl}_3}$, except that 30.0 mg of polymers was used for all binding measurements.

3.9. Selectivity Studies

For cross-reactivity tests, 20 mg of polymer was incubated with 1 mL of 0.8 mM analyte **1**, **17**, **18**, **19** or **20** in CHCl_3 for 1 h. For binary competitive selectivity tests, 20 mg of polymer was incubated with 1 mL of 0.8 mM **1** mixed with 0.8 mM of **17**, **18** or **19** in CHCl_3 for 1 h. The supernatant was analysed by either HPLC for **1**, **18**, **19** and **20** or GC-MS for **17**.

The HPLC method for **1**, **18** and **20** is outlined in Section 3.8.1. Analyte **17** was analysed using a Shimadzu 2010 gas chromatograph coupled to a Shimadzu QP2010 mass spectrometer and a Shimadzu AOC-20s auto sampler. The column was a ZB-5MS capillary column (30 m × 0.25 mm) coated with 0.25 µm of stationary phase. High-purity helium was used as the carrier gas at 71 kPa, with a column flow rate of 1 mL/min, a total flow rate of 9 mL/min and a split ratio of 15. Samples (1 µL) were injected and run using the following program: initial column temperature was 100 °C, which was held for 1 min before increasing to 300 °C at a rate of 10 °C/min. Analyte **19** was analysed using the following HPLC method: The mobile phase consisted of 75% aqueous buffer solution (50 mM K₂HPO₄ adjusted to pH 3.5 with H₃PO₄) and 25% 3:7 H₂O:CH₃CN (with 10 mM TEA). A 10 µL injection volume was used with a run time of 10 min, flow rate of 0.8 mL min⁻¹ and detection wavelength of 190 nm. A calibration curve was generated using solutions in a range from 0.1 to 1 mM.

3.10. Physical Characterisation

3.10.1. Scanning Electron Microscopy

Polymer morphology was examined using a Phillips XL30 scanning electron microscope. The sample was deposited on a sticky carbon tab and coated with gold, using a SPI gold spotter coating unit. SE micrographs of the polymers were obtained at 20,000× magnification at 15.0 kV.

3.10.2. Swelling Measurements

A total of 30 (3) mg of each polymer was packed into an NMR tube, and the height of the dry polymer measured. A solution of **1** (1.00 mL of 0.0800 mM) in acetonitrile or chloroform was added and allowed to soak for 24 h. Polymers were allowed to settle, and the bed height of the swollen polymers was measured. The swelling factor was calculated from the ratio of the bed height of the swollen polymer to the dry polymer.

4. Conclusions

Using self-assembly (non-covalent) and semi-covalent methods, we designed **1**-specific MIPs. In the case of the self-assembly MIPs, a range of potential functional monomers (FM) were screened using a combination of pre-synthetic interaction studies (by molecular modelling and NMR analysis) and binding assays. The best performing self-assembly **1**-MIPs gave IFs of 3 to 7 and were formulated from FM **7** with ethylene glycol dimethacrylate (EGDMA) and trimethylolpropane trimethacrylate (TRIM) crosslinkers, using chloroform as porogen and rebinding solvent at T:FM ratios of 1:1 (E7₁-MIPCHCl₃ and T7₁-MIPCHCl₃) and 1:2 (E7₂-MIPCHCl₃ and T7₂-MIPCHCl₃). The binding parameters K_d and B_{max} were consistent with the MIPs exhibiting a stronger affinity towards **1** (lower K_d), resulting in greater number of binding sites (higher B_{max}) than their corresponding NIPs and observed to be higher for the 1:2 than the 1:1 T:FM formulations. The imprinting effect, as per IFs and NIP/MIP K_d ratios, was observed to be higher for the EGDMA-based MIPs than for the TRIM-based MIPs. The semi-covalent **1**-MIPs were designed using O-4-vinyl 4-benzylpiperazine-1-carbothioate or benzylpiperazine (4-vinylphenyl) carbamate (**16**) as the template–monomer (TM) adduct copolymerized with either EDGMA (E16_{MIPCHCl₃}) or TRIM (T16_{MIPCHCl₃}). We found that **1** could be cleaved from **16** post-polymerisation, leaving a phenol moiety within the imprinted sites capable of hydrogen bonding with **1** upon re-exposure. T16_{MIPCHCl₃} exhibited a greater affinity for **1**—higher IFs, higher binding capacities and lower K_d than E16_{MIPCHCl₃}. The K_d values for semi-covalent MIPs are significantly lower than their self-assembly equivalents, while their B_{max} are, at the most, comparable.

The self-assembly MIPs displayed high levels of cross-reactivity with **19** and **20**, low to moderate with **18** and marginal with **17**. The analytes **17** and **18** are both large molecules that differ in shape, potential and available functional groups to **1** and are therefore a poor fit for the imprinted cavities. In contrast, **19** and **20** are similar in size and chemical

character to **1**, consistent with the observed high cross-reactivity. The semi-covalent MIPs showed similar cross-reactivity trend to the self-assembly MIPs, except for analyte **17**, which recorded high levels of cross-reactivity. The unexpected high cross-reactivity with **17** could possibly be due to its benzoyl group, which is similar in structure and size to the benzyl group of **1**, and could easily fit the imprinted cavities and interact with the phenol moiety. Consistent with the results of the non-competitive cross-reactivity assays, the results of the competitive (binary mixtures) binding studies showed both self-assembly and semi-covalent MIPs to be highly selective towards **1** in the presence of **17**, moderately selective in the presence of **18** but non-selective in the presence of **19**. Competition of **1** with **20** was not studied due to separation problem.

The semi-covalent MIPs were observed to have a stronger affinity for **1** and faster uptake than the self-assembly systems. Both approaches gave MIPs of comparable binding selectivity and cross-reactivity. Overall, the observed IF values were significantly higher with the semi-covalent MIPs than with their self-assembly equivalents; however, it is worth noting that the semi-covalent NIP reference does not contain any FM, thus resulting in minimal **1** binding.

By virtue of its modest selectivity against the test for illicit drugs, **1**-MIP, could potentially be used as a dummy MIP for the broad-based capture and enrichment of illicit substances blended with **1**, e.g., **19** and substituted **20**, for subsequent laboratory analysis. Our preliminary data also demonstrated high affinity for **1** in an aqueous environment, thus raising the possibility for its use in illicit-drug testing.

Supplementary Materials: The supporting information can be downloaded at <https://www.mdpi.com/article/10.3390/ijms24065117/s1>.

Author Contributions: Conceptualization, M.C.B., A.M. and C.I.H.; methodology, K.M.W., M.C.B., A.M. and C.I.H.; validation, M.C.B., A.M. and C.I.H.; formal analysis, K.M.W., M.C.B. and C.I.H.; investigation, K.M.W.; resources, M.C.B., A.M. and C.I.H.; data curation, K.M.W. and C.I.H.; writing—original draft preparation, K.M.W., A.M. and C.I.H.; writing—review and editing, M.C.B., A.M. and C.I.H.; visualization, K.M.W. and C.I.H.; supervision, M.C.B., A.M. and C.I.H.; project administration, M.C.B., A.M. and C.I.H.; funding acquisition, M.C.B., A.M. and C.I.H. All authors have read and agreed to the published version of the manuscript.

Funding: This research was funded by the Australian Research Council and the Australian Federal Police Forensic Services, grant number LP0775378.

Institutional Review Board Statement: Not applicable.

Informed Consent Statement: Not applicable.

Data Availability Statement: Not applicable.

Acknowledgments: The authors acknowledge the Australian Federal Police Forensic Services for providing the illicit drug samples; David Phelan, Monica Rossignoli and Christopher Gordon for their technical assistance with SEM analysis, NMR experiments and organic synthesis.

Conflicts of Interest: The authors declare no conflict of interest. The funders had no role in the design of the study; in the collection, analyses or interpretation of data; in the writing of the manuscript; or in the decision to publish the results.

References

1. Cohen, B.M.Z.; Butler, R. BZP-party pills: A review of research on benzylpiperazine as a recreational drug. *Int. J. Drug Policy* **2011**, *22*, 95–101. [[CrossRef](#)] [[PubMed](#)]
2. Bye, C.; Munro-Faure, A.D.; Peck, A.W.; Young, P.A. A comparison of the effects of 1-benzylpiperazine and dexamphetamine on human performance tests. *Eur. J. Clin. Pharmacol.* **1973**, *6*, 163–169. [[CrossRef](#)] [[PubMed](#)]
3. Campbell, H.; Cline, W.; Evans, M.; Lloyd, J.; Peck, A. Comparison of the effects of dexamphetamine and 1-benzylpiperazine in former addicts. *Eur. J. Clin. Pharmacol.* **1973**, *6*, 170–176. [[CrossRef](#)]

4. Tsutsumi, H.; Katagi, M.; Miki, A.; Shima, N.; Kamata, T.; Nishikawa, M.; Nakajima, K.; Tsuchihashi, H. Development of simultaneous gas chromatography-mass spectrometric and liquid chromatography-electrospray ionization mass spectrometric determination method for the new designer drugs, N-benzylpiperazine (BZP), 1-(3-trifluoromethylphenyl)piperazine (TFMPP) and their main metabolites in urine. *J. Chrom. B Anal. Tech. Biomed. Life Sci.* **2005**, *819*, 315–322.
5. Johnstone, A.C.; Lea, R.A.; Brennan, K.A.; Schenk, S.; Kennedy, M.A.; Fitzmaurice, P.S. Review: Benzylpiperazine: A drug of abuse? *J. Psychopharmacol.* **2007**, *21*, 888–894. [[CrossRef](#)]
6. Gee, P.; Richardson, S.; Woltersdorf, W.; Moore, G. Toxic effects of BZP-based herbal party pills in humans: A prospective study in Christchurch, New Zealand. *N. Z. Med. J.* **2005**, *118*, U1784.
7. Schechter, M.D. Serotonergic-dopaminergic mediation of 3,4-methylenedioxymethamphetamine (MDMA, “ecstasy”). *Pharmacol. Biochem. Behav.* **1988**, *31*, 817–824. [[CrossRef](#)]
8. Wikström, M.; Holmgren, P.; Ahlner, J. A2 (N-Benzylpiperazine) a New Drug of Abuse in Sweden. *J. Anal. Toxicol.* **2004**, *28*, 67–70. [[CrossRef](#)]
9. Luethi, D.; Liechti, M.E. Designer drugs: Mechanism of action and adverse effects. *Arch. Toxicol.* **2020**, *94*, 1085–1133. [[CrossRef](#)]
10. Wilkin, C.; Sweetsur, P.; Parker, K. The impact of the prohibition of benzylpiperazine (BZP) “legal highs” on the availability, price and strength of BZP in New Zealand. *Drug Alcohol Depend.* **2014**, *144*, 47–52. [[CrossRef](#)]
11. De Boer, D.; Bosman, I.J.; Hidvégi, E.; Manzoni, C.; Benkő, A.A.; dos Reys, L.J.A.L.; Maes, R.A.A. Piperazine-like compounds: A new group of designer drug-of-abuse on the European Market. *Forensic Sci. Int.* **2001**, *121*, 47–56. [[CrossRef](#)] [[PubMed](#)]
12. United Nations Office on Drugs and Crime (UNODC). *Recommended Methods for the Identification and Analysis of Piperazines in Seized Materials*; United Nations: New York, NY, USA, 2013; pp. 1–46. Available online: https://www.unodc.org/documents/scientific/STNAR47_Piperazines_Ebook.pdf (accessed on 3 December 2022).
13. Bassindale, T.A.; Berezowski, R. Quantitative analysis of hair samples for 1-benzylpiperazine (BZP) using high-performance liquid chromatography triple quadrupole mass spectrometry (LC-MS/MS) detection. *Anal. Bioanal. Chem.* **2011**, *401*, 2013–2017. [[CrossRef](#)] [[PubMed](#)]
14. Rocha, R.G.; Silva, I.C.O.F.; Arantes, L.C.; Stefano, J.S.; Lima, C.D.; Melo, L.M.A.; Munoz, R.A.A.; dos Santos, W.T.P.; Richter, E.M. Simple and rapid electrochemical detection of 1-benzylpiperazine on carbon screen-printed electrode. *Microchem. J.* **2021**, *167*, 106282. [[CrossRef](#)]
15. Waddell, S.A.; Fernandez, C.; Inverarity, C.C.; Prabhu, R.R. Extending the capability of forensic electrochemistry to the novel psychoactive substance benzylpiperazine. *Sens. Bio-Sens. Res.* **2017**, *13*, 28–39. [[CrossRef](#)]
16. Philp, M.; Shimon, R.; Natasha Stojanovska, N.; Tahtouhb, M.; Shanlin Fu, S. Development and validation of a presumptive colour spot test method for the detection of piperazine analogues in seized illicit materials. *Anal. Methods* **2013**, *5*, 5402–5410. [[CrossRef](#)]
17. Holdsworth, C.I.; Bowyer, M.C.; Lennard, C.; McCluskey, A. Formulation of Cocaine-Imprinted Polymers Utilizing Molecular Modelling and NMR Analysis. *Aus. J. Chem.* **2005**, *58*, 315–320. [[CrossRef](#)]
18. Brisbane, C.; McCluskey, A.; Bowyer, M.; Holdsworth, C.I. Molecularly imprinted films of acrylonitrile/methyl methacrylate/acrylic acid terpolymers: Influence of methyl methacrylate in the binding performance of L-ephedrine imprinted films. *Org. Biomol. Chem.* **2013**, *11*, 2872–2884. [[CrossRef](#)]
19. Xiao, D.; Jiang, Y.; Bi, Y. Molecularly imprinted polymers for the detection of illegal drugs and additives: A review. *Microchim. Acta* **2018**, *185*, 247. [[CrossRef](#)]
20. Mosbach, K.; Ramström, O. The Emerging Technique of Molecular Imprinting and Its Future Impact on Biotechnology. *Nat. Biotechnol.* **1996**, *14*, 163–170. [[CrossRef](#)]
21. Herrera-Chacon, A.; Gonzalez-Calabuig, A.; del Valle, M. Dummy Molecularly Imprinted Polymers Using DNP as a Template Molecule for Explosive Sensing and Nitroaromatic Compound Discrimination. *Chemosensors* **2021**, *9*, 255. [[CrossRef](#)]
22. Haupt, K.; Mosbach, K. Molecularly Imprinted Polymers and Their Use in Biomimetic Sensors. *Chem. Rev.* **2000**, *100*, 2495–2504. [[CrossRef](#)] [[PubMed](#)]
23. Herrera-Chacón, A.; Cetó, X.; del Valle, M. Molecularly imprinted polymers—Towards electrochemical sensors and electronic tongues. *Anal. Bioanal. Chem.* **2021**, *413*, 6117–6140. [[CrossRef](#)] [[PubMed](#)]
24. Scheller, F.W.; Zhang, X.; Yarman, A.; Wollenberger, U.; Gyurcsányi, R.E. Molecularly imprinted polymer-based electrochemical sensors for biopolymers. *Curr. Opin. Electrochem.* **2019**, *14*, 53–59. [[CrossRef](#)]
25. Cui, B.; Liu, P.; Liu, X.; Liu, S.; Zhang, Z. Molecularly imprinted polymers for electrochemical detection and analysis: Progress and perspectives. *J. Mater. Res. Technol.* **2020**, *9*, 12568–12584. [[CrossRef](#)]
26. Wulff, G.; Sarhan, A. The Use of Polymers with Enzyme-Analogous Structures for the Resolution of Racemates. *Angew. Chem. Int. Ed.* **1972**, *11*, 341–344.
27. Brüggemann, O.; Haupt, K.; Ye, L.; Yilmaz, E.; Mosbach, K. New configurations and applications of molecularly imprinted polymers. *J. Chromatogr. A* **2000**, *889*, 15–24. [[CrossRef](#)]
28. Bertolotti, S.G.; Previtali, C.M.; Rufs, A.M.; Encinas, M.V. Riboflavin/Triethanolamine as Photoinitiator System of Vinyl Polymerization. A Mechanistic Study by Laser Flash Photolysis. *Macromolecules* **1999**, *32*, 2920–2924. [[CrossRef](#)]
29. Piletska, E.; Romero-Guerra, M.; Chianella, I.; Karim, K.; Turner, A.; Piletsky, S. Towards the development of multisensor for drugs of abuse based on molecular imprinted polymers. *Anal. Chim. Acta* **2005**, *542*, 111–117. [[CrossRef](#)]

30. Piletsky, S.; Karim, K.; Piletska, E.; Turner, A.; Day, C.; Freebairn, K.; Legge, C. Recognition of ephedrine enantiomers by molecularly imprinted polymers designed using a computational approach. *Analyst* **2001**, *126*, 1826–1830. [[CrossRef](#)]
31. McCluskey, A.; Holdsworth, C.I.; Bowyer, M.C. Molecularly imprinted polymers (MIPs): Sensing, an explosive new opportunity? *Org. Biomol. Chem.* **2007**, *5*, 3233–3244. [[CrossRef](#)]
32. Haupt, K.; Linares, A.V.; Bompert, M.; Bui, B.T. Molecularly imprinted polymers. *Top. Curr. Chem.* **2012**, *325*, 1–28. [[CrossRef](#)]
33. Puoci, F.; Cirillo, G.; Curcio, M.; Parisi, O.I.; Iemma, F.; Picci, N. Molecularly imprinted polymers in drug delivery: State of art and future perspectives. *Expert Opin. Drug Deliv.* **2011**, *8*, 1379–1393. [[CrossRef](#)] [[PubMed](#)]
34. Puoci, F.; Iemma, F.; Picci, N. Stimuli-responsive molecularly imprinted polymers for drug delivery: A review. *Curr. Drug Deliv.* **2008**, *5*, 85–96. [[CrossRef](#)] [[PubMed](#)]
35. Fuchs, Y.; Soppera, O.; Haupt, K. Photopolymerization and photostructuring of molecularly imprinted polymers for sensor applications—A review. *Anal. Chim. Acta* **2012**, *2*, 7–20. [[CrossRef](#)] [[PubMed](#)]
36. Karim, K.; Breton, F.; Rouillon, R.; Piletska, E.V.; Guerreiro, A.; Chianella, I.; Piletsky, S.A. How to find effective functional monomers for effective molecularly imprinted polymers? *Adv. Drug Deliv. Rev.* **2005**, *57*, 1795–1808. [[CrossRef](#)] [[PubMed](#)]
37. Subrahmanyam, S.; Piletsky, S.; Piletska, E.; Chen, B.; Karim, K.; Turner, A.P.F. Bite-and-Switch' approach using computationally designed molecularly imprinted polymers for sensing of creatinine. *Biosens. Bioelectron.* **2001**, *16*, 631–637. [[CrossRef](#)]
38. Breton, F.; Rouillon, R.; Piletska, E.V.; Karim, K.; Guerreiro, A.; Chianella, I.; Piletsky, S.A. Virtual imprinting as a tool to design efficient MIPs for photosynthesis-inhibiting herbicides. *Biosens. Bioelectron.* **2007**, *22*, 1948–1954. [[CrossRef](#)]
39. Pavel, D.; Lagowski, J.; Lepage, C.J. Computationally designed monomers for molecular imprinting of chemical warfare agents—Part V. *Polymer* **2006**, *47*, 8389–8399. [[CrossRef](#)]
40. Williams, D.H.; Cox, J.P.L.; Doig, A.J.; Gardner, M.; Gerhard, U.; Kaye, P.T.; Lal, A.R.; Nicholls, I.A.; Salter, C.J.; Mitchell, R.C. Toward the semiquantitative estimation of binding constants. Guides for peptide-peptide binding in aqueous solution. *J. Am. Chem. Soc.* **1991**, *113*, 7020–7030. [[CrossRef](#)]
41. Nicholls, I.A.; Adbo, K.; Andersson, H.; Andersson, P.; Ankarloo, J.; Hedin-Dahlström, J.; Jokela, P.; Karlsson, J.; Olofsson, L.; Rosengren, J. Can we rationally design molecularly imprinted polymers? *Anal. Chim. Acta* **2001**, *435*, 9–18. [[CrossRef](#)]
42. Sellergren, B.; Lepistoe, M.; Mosbach, K. Highly enantioselective and substrate-selective polymers obtained by molecular imprinting utilizing noncovalent interactions. NMR and chromatographic studies on the nature of recognition. *J. Am. Chem. Soc.* **1988**, *110*, 5853–5860. [[CrossRef](#)]
43. Whitcombe, M.J.; Martin, L.; Vulfson, E.N. Predicting the selectivity of imprinted polymers. *Chromatographia* **1998**, *47*, 457–464. [[CrossRef](#)]
44. Andersson, H.S.; Nicholls, I.A. Spectroscopic evaluation of molecular imprinting polymerization systems. *Bioorg. Chem.* **1997**, *25*, 203–211. [[CrossRef](#)]
45. Ye, L.L.; Mosbach, K. Molecular Imprinting: Synthetic Materials as Substitutes for Biological Antibodies and Receptors. *Chem. Mater.* **2008**, *20*, 859–868. [[CrossRef](#)]
46. Wulff, G. Biorecognition in Molecularly Imprinted Polymers. In *Molecular Interactions in Bioseparations*; Ngo, T.T., Ed.; Springer: Boston, MA, USA, 1993; pp. 363–381.
47. Mosbach, K.; Haupt, K. Some new developments and challenges in non-covalent molecular imprinting technology. *J. Mol. Recognit.* **1998**, *11*, 62–68. [[CrossRef](#)]
48. Harris, T.K.; Mildvan, A.S. High-Precision Measurement of Hydrogen Bond Lengths in Proteins by Nuclear Magnetic Resonance Methods. *Proteins* **1999**, *35*, 275–282. [[CrossRef](#)]
49. Sibrian-Vazquez, M.; Spivak, D.A. Enhanced Enantioselectivity of Molecularly Imprinted Polymers Formulated with Novel Cross-Linking Monomers. *Macromolecules* **2003**, *36*, 5105–5113. [[CrossRef](#)]
50. Spivak, D. Optimization, evaluation, and characterization of molecularly imprinted polymers. *Adv. Drug Deliv. Rev.* **2005**, *57*, 1779–1794. [[CrossRef](#)]
51. Schwarz, L.; Holdsworth, C.I.; McCluskey, A.; Bowyer, M.C. Synthesis and evaluation of a molecularly imprinted polymer selective to 2,4,6-trichlorophenol. *Aust. J. Chem.* **2004**, *57*, 759–764. [[CrossRef](#)]
52. Whitcombe, M.J.; Rodriguez, M.E.; Villar, P.; Vulfson, E.N. A new method for the introduction of recognition site functionality into polymers prepared by molecular imprinting—Synthesis and characterization of polymeric receptors for cholesterol. *J. Am. Chem. Soc.* **1995**, *117*, 7105–7111. [[CrossRef](#)]
53. Kirsch, N.; Alexander, C.; Davies, S.; Whitcombe, M.J. Sacrificial spacer and non-covalent routes toward the molecular imprinting of “poorly-functionalized” N-heterocycles. *Anal. Chim. Acta* **2004**, *504*, 63–71. [[CrossRef](#)]
54. Chunta, S.; Sroysee, W.; Amatatongchai, M.; Lieberzeit, P.A. Molecularly Imprinted Polymers to Detect Profenofos and Carbofuran Selectively with QCM Sensors. *Phys. Med.* **2019**, *7*, 100016.
55. Petcu, M.; Cooney, J.; Cook, C.; Lauren, D.; Schaare, P.; Holland, P. Molecular imprinting of a small substituted phenol of biological importance. *Anal. Chim. Acta* **2001**, *435*, 49–55. [[CrossRef](#)]
56. Booker, K.; Holdsworth, C.I.; Doherty, C.M.; Hill, A.J.; Bowyer, M.C.; McCluskey, A. Ionic liquids as porogens for molecularly imprinted polymers: Propranolol, a model study. *Org. Biomol. Chem.* **2014**, *12*, 7201–7210. [[CrossRef](#)]
57. Booker, K.; Bowyer, M.C.; Holdsworth, C.I.; McCluskey, A. Efficient preparation and improved sensitivity of molecularly imprinted polymers using room temperature ionic liquids. *Chem. Commun.* **2006**, 1730–1732. [[CrossRef](#)]

58. Schwarz, L.; Bowyer, M.C.; Holdsworth, C.I.; McCluskey, M.C. Synthesis and Evaluation of a Molecularly Imprinted Polymer Selective to 2,4,6-Trichloroanisole. *Aust. J. Chem.* **2006**, *59*, 129–134. [[CrossRef](#)]
59. Pardo, A.; Mespouille, L.; Blankert, B.; Trouillas, P.; Surin, M.; Dubois, P.; Duez, P. Quercetin-imprinted chromatographic sorbents revisited: Optimization of synthesis and rebinding protocols for application to natural resources. *J. Chromatogr. A* **2014**, *1364*, 128–139. [[CrossRef](#)]
60. Abu-Alsoud, G.F.; Hawboldt, K.A.; Bottaro, C.S. Comparison of Four Adsorption Isotherm Models for Characterizing Molecular Recognition of Individual Phenolic Compounds in Porous Tailor-Made Molecularly Imprinted Polymer Films. *ACS Appl. Mater. Interfaces* **2020**, *12*, 11998–12009. [[CrossRef](#)]
61. Rajkumar, R.; Warsinke, A.; Möhwald, H.; Scheller, F.W.; Katterle, M. Analysis of recognition of fructose by imprinted polymers. *Talanta* **2008**, *76*, 1119–1123. [[CrossRef](#)]
62. Muhammad, T.; Nur, Z.; Piletska, E.V.; Yimit, O.; Piletsky, S.A. Rational design of molecularly imprinted polymer: The choice of cross-linker. *Analyst* **2012**, *137*, 2623–2628. [[CrossRef](#)]
63. Turner, N.W.; Holmes, N.; Brisbane, C.; McGeachie, A.B.; Bowyer, M.C.; McCluskey, A.; Holdsworth, C.I. Effect of template on the formation of phase-inversed molecularly imprinted polymer thin films: An assessment. *Soft Matter* **2009**, *5*, 3663–3671. [[CrossRef](#)]
64. Cole, M.; Baron, M. Drugs of Abuse. In *Crime Scene to Court: The Essentials of Forensic Science*, 4th ed.; White, P.C., Ed.; The Royal Society of Chemistry UK: Cambridge, UK, 2016; pp. 401–443.
65. European Monitoring Centre for Drugs and Drug Addiction. BZP/Piperazines Drug Profile. Available online: <https://www.emcdda.europa.eu/publications/drug-profiles/bzp> (accessed on 15 February 2023).
66. UN International Drug Control Programme. *Drug Characterization/Impurity Profiling—Background and Concepts*; United Nations: New York, NY, USA, 2001; pp. 1–19. Available online: <https://digitallibrary.un.org/record/454230?ln=en> (accessed on 15 February 2023).
67. Patel, J.R.; Patel, K.H.; Patel, R.M. Reactivity ratio of novel acrylic copolymer by NMR spectroscopy. *Colloid Polym. Sci.* **2009**, *287*, 89–95. [[CrossRef](#)]
68. Corson, B.B.; Heintzelman, W.J.; Schwartzman, L.H.; Tiefenthal, H.E.; Lokken, R.J.; Nickels, J.E.; Atwood, G.R.; Pavlik, F.J. Preparation of Vinylphenols and Isopropenylphenols. *J. Org. Chem.* **1958**, *23*, 544–549. [[CrossRef](#)]
69. Oh, H.K.; Ha, J.S.; Sung, D.D.; Lee, I. Aminolysis of Aryl Chlorothionoformates with Anilines in Acetonitrile: Effects of Amine Nature and Solvent on the Mechanism. *J. Org. Chem.* **2004**, *69*, 8219–8223. [[CrossRef](#)]

Disclaimer/Publisher’s Note: The statements, opinions and data contained in all publications are solely those of the individual author(s) and contributor(s) and not of MDPI and/or the editor(s). MDPI and/or the editor(s) disclaim responsibility for any injury to people or property resulting from any ideas, methods, instructions or products referred to in the content.